文章编号: 1001－2060(2008)02－0144－04

基于改进型不变线矩特征的机组轴心轨迹形状自动识别

万书亭[1], 吴炳胜[2]
(1. 华北电力大学 机械工程学院, 河北 保定 071003; 2. 河北工程大学 机电工程学院, 河北 邯郸 056038)

摘　要: 提出了一种改进型不变线矩, 给出了详细的数学表达式和满足平移、旋转、伸缩不变性的证明过程, 并又提出了一种基于改进型不变线矩的轴心轨迹形状自动识别新方法, 将采集的两相互垂直方向的振动位移信号, 经消噪处理拟合为轴心轨迹, 采用改进型不变线矩代替传统的 HU 氏不变面矩, 计算不变线矩特征向量。将仿真生成的各种轴心轨迹不变线矩特征向量作为参考模式, 利用关联度识别实际检测的轴心轨迹, 成功识别了 MJF-30-6 型发电机组 3 种工况的轴心轨迹形状。

关　键　词: 发电机组; 轴心轨迹; 不变线矩; 关联度; 自动识别
中图分类号: TM312　　文献标识码: A

引　言

汽轮发电机组振动状态监测是机组运行监测中非常重要内容之一, 而轴心轨迹是反映机组转子振动状态的特征量, 从一个侧面反映着转子运动状态或故障的基本信息, 比如不平衡故障使轴心轨迹呈椭圆形, 不对中故障使轴心轨迹呈外 8 字形, 油膜涡动故障使轴心轨迹呈内 8 字形等。传统的人工识别轴心轨迹方法严重影响了故障诊断的自动化水平, 因此如何自动识别轴心轨迹形状具有重要的现实意义。轴心轨迹形状的自动识别问题实质是二维图像的模式识别问题。在图像识别领域, Ming-kuei HU 于 1962 年提出了具有旋转、平移、缩放不变性的 7 个不变面矩, 并得到了广泛的应用[1~5], 文献[4]提出了先利用边界颜色填充轴心轨迹内部, 将轴心轨迹线图转化为图象, 然后再利用不变面矩特征识别轴心轨迹。但是对于简单的轴心轨迹, 可以用边界颜色填充转变为实体图像识别, 而对于复杂的轴心轨迹很难判断边界及其颜色。实际上机组轴心轨迹图形是一条二维矢量曲线, 大多数情况下并不是封闭的, 形状可能规则也可能不规则, 轨迹的圈数也是不定的, 基于这些因素, 采用不变线矩的线积分来代替不变面矩的面积分更接近实际情况。

首先分析了轴心轨迹线图的不变线矩计算方法, 指出在离散情况下传统的不变线矩计算方法不满足伸缩不变性, 然后提出了一种改进型不变线矩, 并给出了详细的数学表达式和满足平移、旋转、伸缩不变性的证明过程。在此基础上又提出了一种基于此改进型不变线矩的发电机组轴心轨迹形状自动识别新方法, 最后实测并自动识别了 MJF－30－6 型发电机组转子在空转、空载运行、并网正常运行 3 种工况的轴心轨迹形状。

1　线矩及其不变性[6]

设轴心轨迹由 n 个离散的数据点组成, 定义离散化的 $p+q$ 阶矩 m_{pq} 为:

$$m_{pq}=\sum_{i=0}^{n-1}x^p y^q \Delta S_i \quad p, q=0, 1, 2, 3, \Lambda \tag{1}$$

式中: $\Delta S_i=\sqrt{(x_i-x_{i-1})^2+(y_i-y_{i-1})^2}$, $f(x, y)$ 为图象在坐标点 (x, y) 上的灰度, 对于轴心轨迹, 认为其经过的各点的灰度相同, 即取 $f(x, y)=1$, 没有经过的各点灰度为零, 即 $f(x, y)=0$。

满足平移不变性离散化的中心矩:

$$\mu_{pq}=\sum_{i=0}^{n-1}(x-\bar{x})^p (y-\bar{y})^q \Delta S_i \quad p, q=0, 1, 2, 3, \Lambda \tag{2}$$

式中: $(\bar{x}, \bar{y})$ 代表图形的质心, $\begin{cases}\bar{x}=m_{10}/m_{00}\\ \bar{y}=m_{01}/m_{00}\end{cases}$。

对 μ_{pq} 进行正规化处理得到 η_{pq}, 它满足图形的平移和伸缩不变性:

$$\eta_{pq}=\frac{\mu_{pq}}{\mu_{00}^{1+(p+q)/2}} \quad p+q\geqslant 2 \quad p, q=0, 1, 2, 3, \Lambda \tag{3}$$

收稿日期: 2007－03－01;　修订日期: 2007－08－22
基金项目: 国家自然科学基金资助项目(50677017)
作者简介: 万书亭(1970－), 男, 山西长治人, 华北电力大学副教授, 博士。

?1994-2018 China Academic Journal Electronic Publishing House. All rights reserved.　http://www.cnki.net

HU 通过研究得到了 $p+q\leqslant 3$ 的 7 个不变矩 $\varphi_1 \sim \varphi_7$:

$$\begin{cases}\varphi_1=\eta_{20}+\eta_{02}\\ \varphi_2=(\eta_{20}-\eta_{02})^2+4\eta_{11}^2\\ \varphi_3=(\eta_{30}-3\eta_{12})^2+(3\eta_{21}-\eta_{03})^2\\ \varphi_4=(\eta_{30}+\eta_{12})^2+(\eta_{21}+\eta_{03})^2\\ \varphi_5=(\eta_{30}-3\eta_{12})(\eta_{30}+\eta_{12})[(\eta_{30}+\eta_{12})^2-3(\eta_{21}+\eta_{03})^2]+\\ \quad(\eta_{21}-\eta_{03})(\eta_{21}+\eta_{03})[3(\eta_{30}+\eta_{12})^2-(\eta_{21}+\eta_{03})^2]\\ \varphi_6=(\eta_{20}-\eta_{02})[(\eta_{30}+\eta_{12})^2-(\eta_{21}+\eta_{03})^2]+\\ \quad 4\eta_{11}(\eta_{30}+\eta_{12})(\eta_{21}+\eta_{03})\\ \varphi_7=(3\eta_{21}-\eta_{03})(\eta_{30}+\eta_{12})[(\eta_{30}+\eta_{12})^2-3(\eta_{21}+\eta_{03})^2]+\\ \quad(3\eta_{12}-\eta_{30})(\eta_{21}+\eta_{03})[3(\eta_{30}+\eta_{12})^2-(\eta_{21}+\eta_{03})^2]\end{cases} \tag{4}$$

式中: φ_1 是图形发散程度的度量指标, 图形的发散程度越大, φ_1 越大; φ_2 表示图形对称性的度量指标, 图形对称性越好, φ_2 越小。

2　改进型不变线矩及其计算方法

2.1　离散情况下 HU 不变线矩伸缩可变性分析

由于测量得到的轴心轨迹线图是一些离散的数据点, 可以证明式(4)所定义的 7 个不变矩满足平移、旋转不变性(由于篇幅所限, 证明省略), 但不满足伸缩不变性, 证明如下:

设比例因子为 ρ, 则发生伸缩变化后的坐标点为 x'和y', 有:

$$\begin{cases}x'=\rho x\\ y'=\rho y\end{cases} \tag{5}$$

图形进行伸缩后:

$$\Delta S'_i=\sqrt{(\rho x_i-\rho x_{i-1})^2+(\rho x_i-\rho x_{i-1})^2}=\rho\Delta S_i \tag{6}$$

伸缩后中心矩 μ'_{pq}的因子:

$$x'_i-\bar{x}'=\rho x_i-\frac{m'_{10}}{m'_{00}}=\rho x_i-\sum_{i=1}^{n-1}\rho x_i\rho\Delta S_i/\sum_{i=1}^{n-1}\rho\Delta S_i=\rho x_i-\rho\sum_{i=1}^{n-1}x_i\Delta S_i/\sum_{i=1}^{n-1}\Delta S_i=\rho x_i-\rho\bar{x}=\rho(x_i-\bar{x}) \tag{7}$$

$$y'_i-\bar{y}'=\rho(y_i-\bar{y})$$

所以, 伸缩后中心矩 μ'_{pq}:

$$\mu'_{pq}=\sum_{i=1}^{n-1}[\rho(x_i-\bar{x})]^p[\rho(y_i-\bar{y})]^q\rho\Delta S_i=\rho^{1+p+q}\mu_{pq} \tag{8}$$

正规化的中心矩 η'_{pq}:

$$\eta'_{pq}=\frac{\mu'_{pq}}{\mu'^{1+(p+q)/2}_{00}}=\rho^{(p+q)/2}\eta_{pq} \tag{9}$$

可见, 在图形进行伸缩以后的中心矩与因子 $\rho^{(p+q)/2}$有关, 即不能保证对图形比例缩放的不变性。

2.2　改进型不变线矩及其计算方法

考察 7 个不变线矩, 设经比例缩放之后的不变线矩为 φ'_i, 由式(9)可得到:

$$\varphi'_1=\rho^{2/2}\eta_{20}+\rho^{2/2}\eta_{02}=\rho\varphi_1$$

$$\varphi'_2=(\rho^{2/2})^2(\eta_{20}-\eta_{02})^2+4(\rho^{2/2})^2\eta_{11}^2=\rho^2\varphi_2$$

$$\varphi'_3=(\rho^{3/2})^2(\eta_{30}-3\eta_{12})^2+(\rho^{3/2})^2(3\eta_{21}-\eta_{03})^2=\rho^3\varphi_3$$

$$\varphi'_4=(\rho^{3/2})^2(\eta_{30}+\eta_{12})^2+(\rho^{3/2})^2(\eta_{21}+\eta_{03})^2=\rho^3\varphi_4$$

$$\varphi'_5=\rho^{3/2}(\eta_{30}-3\eta_{12})\rho^{3/2}(\eta_{30}+\eta_{12})(\rho^{3/2})^2\times[(\eta_{30}+\eta_{12})^2-3(\eta_{21}+\eta_{03})^2]+\rho^{3/2}(3\eta_{21}-\eta_{03})\rho^{3/2}\times(\eta_{21}+\eta_{03})(\rho^{3/2})^2[3(\eta_{30}+\eta_{12})^2-(\eta_{21}+\eta_{03})^2]=\rho^{3/2}\rho^{3/2}(\rho^{3/2})^2\varphi_5=\rho^6\varphi_5$$

$$\varphi'_6=\rho^{2/2}(\eta_{20}-\eta_{02})(\rho^{3/2})^2[(\eta_{30}+\eta_{12})^2-(\eta_{21}+\eta_{03})^2]+4\rho^{2/2}\eta_{11}\rho^{3/2}(\eta_{30}+\eta_{12})\rho^{3/2}(\eta_{21}+\eta_{03})=\rho^4\varphi_6$$

$$\varphi'_7=\rho^{3/2}(3\eta_{21}-\eta_{03})\rho^{3/2}(\eta_{30}+\eta_{12})(\rho^{3/2})^2\times[(\eta_{30}+\eta_{12})^2-3(\eta_{21}+\eta_{03})^2]+\rho^{3/2}(3\eta_{12}-\eta_{30})\rho^{3/2}(\eta_{21}+\eta_{03})(\rho^{3/2})^2[3(\eta_{30}+\eta_{12})^2-(\eta_{21}+\eta_{03})^2]=\rho^{3/2}\rho^{3/2}(\rho^{3/2})^2=\rho^6\varphi_7 \tag{10}$$

为了消除比例因子的影响, 根据式(10), 以 φ'_2 为基础, 构造以下函数:

$$\begin{aligned}M_1&=\varphi'^2_1/\varphi'_2=(\rho\varphi_1)^2/\rho^2\varphi_2=\varphi_1^2/\varphi_2\\ M_3&=\varphi'^2_3/\varphi'^3_2=(\rho^3\varphi_3)^2/(\rho^2\varphi_2)^3=\varphi_3^2/\varphi_2^3\\ M_4&=\varphi'^2_4/\varphi'^3_2=(\rho^3\varphi_4)^2/(\rho^2\varphi_2)^3=\varphi_4^2/\varphi_2^3\\ M_5&=\varphi'_5/\varphi'^3_2=(\rho^6\varphi_5)/(\rho^2\varphi_2)^3=\varphi_5/\varphi_2^3\\ M_6&=\varphi'_6/\varphi'^2_2=(\rho^4\varphi_6)/(\rho^2\varphi_2)^2=\varphi_6/\varphi_2^2\\ M_7&=\varphi'_7/\varphi'^3_2=(\rho^6\varphi_7)/(\rho^2\varphi_2)^3=\varphi_7/\varphi_2^3\end{aligned} \tag{11}$$

构造后函数 M_i 的表达式已经消除了比例因子 ρ 的影响, 因此对图形的比例伸缩可以保持不变性, 同时由于原不变线矩 φ_i 本身具有平移和旋转的不变性, 构造后的 M_i 也同时具有平移和旋转不变性, 从而可以用 M_i 进行轴心轨迹形状的识别。

3　基于改进型不变线矩特征的机组轴心轨迹形状自动识别

3.1　轴心轨迹形状识别的参考模式建立

轴心轨迹形状的参考模式的建立是轴心轨迹识别的难点, 因为不同的故障对应着不同的轴心轨迹图形, 并且对同一种故障, 随着这种故障振动的幅

?1994-2018 China Academic Journal Electronic Publishing House. All rights reserved.　http://www.cnki.net

值、初相角不同，轴心轨迹图形的变形程度也不同，计算得到的不变线矩也不相同，有时甚至相差很大，这给图形的识别带来了一定的困难。常见的几种轴心轨迹图形不变线矩如表 1 所示。

表 1 参考模式的不变线矩

模式编号	轴心轨迹图形	改进后的不变线矩					
		M_1	M_3	M_4	M_5	M_6	M_7
1	圆	20.862 6	20.862 9	20.862 4	20.862 5	10.431 2	−2.024 3
2	椭圆	1.972 34	−44.132 4	−40.296 5	−41.255 6	−20.148 3	−46.658 7
3	香蕉形(1)	1.583 3	3.289 9	−2.449 7	−1.114 7	−1.260 4	−1.869
4	香蕉形(2)	6.132 6	16.986 7	11.518 8	12.724	5.393 2	12.242 8
5	外 8 字(1)	2.864 1	3.429 9	−0.835 9	−2.204 8	−1.408 6	0.161 6
6	外 8 字(2)	0.059 9	−7.479 1	−9.027 1	−9.366 7	−5.011 6	−10.962 2
7	外 8 字(3)	4.596 9	10.978 7	7.090 7	7.879 1	3.544 9	7.472 8
8	内 8 字(1)	3.628 6	−3.325 6	4.670 5	2.642 5	2.144 3	1.159 5
9	内 8 字(2)	2.071 9	−3.502	3.384 3	−3.413 7	−1.692 3	−0.507 5
10	内 8 字(3)	2.166 9	−0.031 2	0.321 2	0.184 2	−0.132 8	−0.953 8
11	梅花形(1)	2.117 0	0.277 3	−3.151 6	−3.180 3	−1.576 9	−0.563 0
12	梅花形(2)	2.129 0	0.650 6	1.958 3	1.630 5	0.935 5	−1.548 6

3.2 基于关联度的轴心轨迹形状识别方法

3.2.1 实测轴心轨迹的不变矩

在模拟发电机 MJF−30−6 上实测转子的轴心轨迹。模拟发电机额定电压 U_N=400 V、额定转速 n_N=1 000 r/min，由 Z2−91 型直流电动机拖动。图 1(a)为发电机空转时的轴心轨迹，(b)为发电机空载运行时的轴心轨迹，(c)为发电机在额定工况并网正常运行时的轴心轨迹，这 3 个轴心轨迹都经小波软阈值消噪处理，表 2 为计算得到的不变线矩。

表 2 待识别模式的不变线矩

待识别模式	改进后的不变线矩					
	M_1	M_3	M_4	M_5	M_6	M_7
图 1(a)	0.028 1	−3.568 8	−6.170 4	−5.561 6	−4.484 6	−6.784 7
图 1(b)	0.023 4	−1.831 3	−1.907 1	−1.888 2	−0.966 3	−9.572 7
图 1(c)	2.120 5	0.602 7	1.854 0	1.605 2	0.853 2	−1.636 7

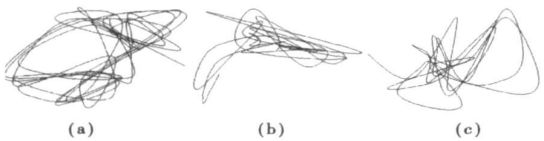

图 1 MJF−30−6 发电机转子振动轴心轨迹图形

3.2.2 关联度计算

关联度分析方法是灰色系统关联性的主要表现，由于计算量小被广泛应用于故障诊断中，本文采用文献[4]提出的新型关联度计算方法。

设 $X_0=\{x_0(j)\}$，$j=1,2,\cdots,n$ 为待识别模式序列，$X_i=\{x_i(j)\}$，$i=1,2,\cdots,m$，$j=1,2,\cdots n$ 为参考模式序列，则 X_0 与 X_i 的关联系数为：

$$\gamma(x_0(j),x_i(j))=\frac{\min\limits_i\min\limits_j|x_0(j)-x_i(j)|+\rho\max\limits_i\max\limits_j|x_0(j)-x_i(j)|}{|x_0(j)-x_i(j)|+\rho\max\limits_i\max\limits_j|x_0(j)-x_i(j)|} \tag{12}$$

式中：分辨系数 $\rho\in[0,1]$ 为取定的常数。

记 $\beta_i(j)=\gamma(x_0(j),x_i(j))$，则关联系数矩阵为：

$$\beta=\begin{bmatrix}\beta_1(1) & \beta_1(2) & \cdots & \beta_1(n)\\ \beta_2(1) & \beta_2(2) & \cdots & \beta_2(n)\\ \vdots & \vdots & & \vdots\\ \beta_m(1) & \beta_m(2) & \cdots & \beta_m(n)\end{bmatrix} \tag{13}$$

记 $\beta_{\max}(j)=\max\limits_i\beta_i(j)$，即 β 矩阵中每一列最大值，为最大关联系数阵。$\beta_{\min}(j)=\min\limits_i\beta_i(j)$，即 β 矩阵中每一列最小值，为最小关联系数阵。记 $D=\sqrt{\sum_{j=1}^{n}(\beta_{\max}(j)-\beta_{\min}(j))^2}$ 为关联系数间最大距离，设 $d_i=\sqrt{\sum_{j=1}^{n}(\beta_i(j)-\beta_{\min}(j))^2}$，则定义关联度计算式为：

$$\gamma_i=d_i/D \tag{14}$$

关联度 γ_i 的大小反应 X_0 与 X_i 的关联程度，利

?1994-2016 China Academic Journal Electronic Publishing House. All rights reserved. http://www.cnki.net

用 γ_i 的大小可以对系统故障模式进行识别。计算得到的关联度值如表 3 所示（$\rho=0.5$）。

表 3　待识别模式与参考模式间的关联度

参考模式编号	发电机运行状况		
	工况(a)	工况(b)	工况(c)
1(圆)	0.383 9	0.330 1	0.512 7
2(椭圆)	0.324 1	0.295 9	0.304 5
3(香蕉形 1)	0.817 6	0.885 1	0.867 7
4(香蕉形 2)	0.354 2	0.402 0	0.509 4
5(外 8 字 1)	0.778 7	0.859 6	0.846 0
6(外 8 字 2)	0.924 0	0.783 1	0.580 2
7(外 8 字 3)	0.474 0	0.529 5	0.659 1
8(内 8 字 1)	0.751 5	0.748 4	0.854 7
9(内 8 字 2)	0.880 4	0.839 5	0.850 5
10(内 8 字 3)	0.240 5	0.213 1	0.489 4
11(梅花形 1)	0.866 1	0.882 8	0.864 5
12(梅花形 2)	0.751 3	0.807 6	0.999 8
识别结果	外 8 字形	不确定	梅花形

以最大关联度为轴心轨迹形状识别结果，图 1(a)所示轴心轨迹为外 8 字形(转子轴承振动的 2 倍转频分量较大，初步确定为轴系对中不好)；(b)所示轴心轨迹比较紊乱，与参考模式 3(香蕉形)、5(外 8 字)、9(内 8 字)、11(梅花形)的关联度差别很小，因此识别结果不确定；(c)所示轴心轨迹比较清楚，识别为梅花形。

4　结　论

(1) 针对发电机组振动轴心轨迹的二维离散线图，指出了传统的不变线矩虽满足平移、旋转不变性，但不满足伸缩不变性。为此提出了一种同时满足平移、伸缩、旋转不变性的改进型不变线矩，并且与传统的 HU 不变面矩相比，由于用不变线矩的单重积分代替 HU 不变面矩的双重积分运算，减少了乘方运算的次数，从而提高运算速度和精度。

(2) 建立了基于改进型不变线矩特征的机组轴心轨迹形状自动识别方法，并成功识别了 MJF－30－6 型发电机组转子在空转、空载运行、并网正常运行 3 种工况的轴心轨迹形状。

本研究项目还得到 2006 年华北电力大学博士学位教师科研基金资助。

参考文献：

[1] 李友平，陈启卷. 基于灰色理论与不变性矩的水电机组轴心轨迹自动识别[J]. 电力系统自动化，2001，25(9)：19－22.

[2] 韩西京，李录平，史铁林，等. 旋转机械轴心轨迹的自动识别[J]. 振动、测试与诊断，1997，17(3)：20－25.

[3] 倪传坤，周建中，付　波. 基于改进不变矩的发电机轴心轨迹识别[J]. 电力科学与工程，2004(2)：16－18.

[4] 万书亭，李和明，李永刚. 基于不变矩特征和新型关联度的轴心轨迹形状自动识别[J]. 热能动力工程，2005，20(3)：239－241，245.

[5] 张新江，李　奕，杨建国. 汽轮发电机组轴心轨迹特征的自动提取及辨识[J]. 热能动力工程，1999，14(6)：487－488.

[6] 王　海，郑莉媛. 水轮发电机组轴心轨迹自动识别方法研究[J]. 水力发电学报，2002，8：73－80.

（编辑　伟）

新技术、新工艺

汽轮机装置改造的技术措施

《Электрические станции》2005 年 10 月号介绍了 ЛМЗ(列宁格勒金属工厂)在最近 10～15 年期间为了提高现有机组的可靠性、经济性、机动性、简化运行条件所制定的先进工艺和改造措施。

这些措施包括改进汽轮机中压缸的前端密封，改造汽轮机端部密封系统，利用加热空气对汽轮机装置的设备进行油封，改造汽轮机高压缸和中压缸法兰的加热系统，在进汽区域内高压缸和中压金属温度为 250～270 ℃时水处理装置和润滑系统更早停机的工艺，汽轮机从冷态启动和真空系统密封性检查的工艺，在从热力系统除去止回阀的情况下到网路加热器的抽汽管道的改造，通过汽轮机低压缸关闭的转动隔板的蒸汽流量估算的工艺，进行转动隔板的密封，在从热力系统除去内装的第一级低压加热器情况下汽轮机装置的改造。

应该指出，不仅在现有的机组上，而且在设计新的汽轮机装置时，都可成功地应用本文所介绍的一些技术方案。

（吉桂明　供稿）

?1994-2018 China Academic Journal Electronic Publishing House. All rights reserved.　http://www.cnki.net

In the light of the huge amount of time-consuming CFD (computational fluid dynamics) calculations during the numerical optimization of a turbo-machinery unit, developed was an optimized design method based on an approximate model. The keystone of the method under discussion consists of a sample database used for establishing an approximate model between the sample-point-based geometrical information and its performance. The optimization method has been applied to the optimized design of centrifugal compressor blades. With a maximized isentropic efficiency serving as an objective function and under the condition of keeping the flow rate and total pressure ratio not being decreased, the isentropic efficiency of the impeller has been increased by 2.7% after the optimization. Moreover, the optimized blade profile became more straight and flat, and the blade tip profile underwent a more conspicuous change than that of the blade hub profile. **Key words**: compressor, optimized design, blade, approximate model

考虑主蒸汽压力变化的机组一次调频动态特性= **Dynamic Characteristics of the Primary Frequency Modulation of a Turbo-generator under a Due Consideration of Main Steam Pressure Variation**[刊, 汉] / LIU Xiao-qiang (Automation Control Center, Shanghai Steam Turbine Co. Ltd., Shanghai, China, Post Code: 200240), WANG Xi-tian (Department of Electrical Engineering, Shanghai Jiaotong University, Shanghai, China, Post Code: 200240)// Journal of Engineering for Thermal Energy &Power. —2008, 23(2). —140 ~ 143

During the study of dynamic characteristics of primary frequency modulation it is usually supposed that the boiler in a power plant has sufficient large heat-storage capacity to keep main steam pressure constant and its flow rate in direct proportion to the valve opening degree. In practice, however, the boiler heat-storage capacity is always limited. When the heat stored in the boiler is used up or the main steam pressure changes with the valve opening degree, the primary frequency modulation will be somewhat affected. The authors have established a model showing the influence of main steam pressure change on the primary frequency modulation characteristics of a turbo-generator unit, and conducted a simulation analysis respectively in the frequency and time domains. The research results show that the characteristics in question have a relatively small difference in the high frequency band, but a conspicuous one in the low frequency band. An excessively small low-frequency gain may evidently result from the primary frequency modulation when the main steam pressure is considered as dynamic, which is unfavorable for the control of the relatively low frequency and long-time grid cycle-wave variation. As a result, such a phenomenon as the falling of primary-frequency modulation output power leading to a deviation from the ideal design performance may occur after a certain period of time. To enhance the frequency modulation performance, it is necessary to rationally configure the CCS (coordinated control system) and coordinate the primary and secondary frequency modulation. **Key words**: turbo-generator, primary frequency modulation, dynamic characteristics, main steam pressure

基于改进型不变线矩特征的机组轴心轨迹形状自动识别= **Automatic Identification of Plant Axial Trajectory Shapes Based on Improved Invariant Linear-moment Characteristics**[刊, 汉] / WAN Shu-ting (Education Ministry Key Laboratory on Power Plant Equipment Condition Monitoring and Control, College of Mechanical Engineering, North China Electric Power University, Baoding, China, Post Code: 071003), WU Bing-sheng (College of Electro-mechanical Engineering, Hebei Engineering University, Handan, China, Post Code: 056038)// Journal of Engineering for Thermal Energy &Power. — 2008, 23(2). —144 ~ 147

Presented was an improved invariant linear-moment algorithm with a detailed mathematical expression and a demonstration process featuring an invariance that satisfies plant movement, rotation, elongation and compression. Furthermore, a novel

?1994-2018 China Academic Journal Electronic Publishing House. All rights reserved. http://www.cnki.net

method for the automatic identification of axial trajectory shapes based on improved invariant linear-moment characteristics was put forward, enabling two collected mutually vertical vibration displacement signals to be fitted through a noise treatment into axial trajectories. Improved invariant linear-moments have been adopted to replace a traditional HU's invariable surface moment to calculate the invariant linear-moment eigenvector. With invariant linear-moment eigenvectors of various axial trajectories produced in the simulation process serving as reference modes, the authors have employed correlation to identify the axial trajectory actually tested, and successfully identified the axial trajectory shapes of MJF-30-6 model turbogenerator unit under three different operating conditions. **Key words**: power generator unit, axial trajectory, invariant linear moment, correlation, automatic identification

复杂循环船用燃气轮机间冷器的数值模拟＝**Numerical Simulation of an Intercooler for a Complex-cycle Marine Gas Turbine**[刊, 汉] / LI Zhuo, ZHANG Hui-bing, WEN Xue-you, et al (CSIC No. 703 Research Institute, Harbin, China, Post Code: 150036) // Journal of Engineering for Thermal Energy & Power. — 2008, 23(2). —148 ~ 152

In an IC (intercooling) cycle gas turbine, intercoolers are components that exercise a major influence on the gas turbine performance. To determine the structural type of the intercoolers to be installed on gas turbines, three intercooler structural schemes have been proposed for a marine gas turbine and a numerical simulation has been performed. Through optimization, relatively good simulation results were obtained. Due to the simplification of a model during the calculation, the pressure-drop loss calculation result is not accurate enough. Consequently, a small flow-passage simulation calculation has been additionally conducted with the pressure-drop loss calculation results in the three schemes being revised. **Key words**: gas turbine, intercooler, intercooling recuperator (ICR) cycle, intercooling (IC) cycle

线性唯象传热规律下复杂系统的热力学优化＝**Thermodynamic Optimization of a Complex System under a Linear Phenomenological Heat Transfer Law**[刊, 汉] / LI Jun, CHEN Lin-gen, SUN Feng-rui (Postgraduate School, Naval University of Engineering, Wuhan, China, Post Code: 430033) // Journal of Engineering for Thermal Energy & Power. — 2008, 23(2). —153 ~ 156

A real heat transfer process does not always follow Newton's heat transfer law and the heat transfer law, however, exercise an enormous influence on the thermodynamic cycle performance. The authors have utilized a commonly used heat transfer law in non-equilibrium thermodynamics, namely, a linear phenomenological heat transfer law, to study a complex system. The latter involves several heat sources at different temperatures, a finite heat capacitance sub-system and a transformer (heat engine or refrigerator). The optimum temperature of the working medium of the transformer and the optimum free temperature of the sub-system have been obtained by using Lagrange Equation. The corresponding maximum power output of the system has also been determined and compared with that calculated by using Newton's heat transfer law. The calculation method under discussion can provide an approach for the calculation of the real temperature distribution and energy limits of a practical complex system. **Key words**: linear phenomenology, heat transfer law, complex system, thermodynamic optimization

螺旋助片自支撑换热器强化换热试验研究＝**An Experimental Study of Intensified Heat Exchange of a Spiral-finned Self-supported Heat Exchanger**[刊, 汉] / WU Jin-xing, ZHU Deng-liang, WEI Xin-li, et al (Energy-saving Technology Research Center, Zhengzhou University, Zhengzhou, China, Post Code: 450001) // Journal of Engineering for Thermal Energy & Power. —2008, 23(2). —157 ~ 160

?1994-2018 China Academic Journal Electronic Publishing House. All rights reserved. http://www.cnki.net